PROCEEDINGS, Twenty-Fifth Workshop on Geothermal Reservoir Engineering
Stanford University, Stanford, California, January 24-26, 2000
SGP-TR-165

A REVIEW OF EXPLORATION GAS GEOTHERMOMETRY

Thomas Powell

Thermochem, Inc.
3414 Regional Parkway
Santa Rosa, CA 95403

ABSTRACT

Like their liquid counterparts, gas geothermometers are based upon either empirical or thermodynamic equations for chemical reactions thought to equilibrate in geothermal reservoirs. Presentations of geothermometer results take three different general forms: equations, y–T grids and gas ratio grids. Among the thermodynamics-based geothermometers, the H_2, CO, HSH, H_2S, CO_2 and CO_2–H_2 geothermometer reactions appear to equilibrate at usual reservoir conditions, but the Fischer-Tropsch and NAH geothermometer reactions are likely too slow. Empirical geothermometers have been proposed for a number of gas combinations, but they either do not provide an advantage over their thermodynamic counterparts or, in the case of the DAP geothermometer, do not perform as expected.

The y–T gas grid geothermometers employ a combination of two geothermometer reactions to allow the simultaneous determination of y (the fraction of a hypothetical equilibrated reservoir steam) and temperature. Processes that modify fumarole gas concentrations, such as reservoir boiling and near surface condensation adversely affect y–T grid results, limiting their application. They also suffer from uncertainty as to the appropriateness of the y model to a particular steam source.

Gas ratio grids overcome some of these difficulties by fixing hydrogen fugacities through the assumption of a single redox state for the system, and by using argon concentration as a proxy for P_{H2O}. They suffer from ambiguities with respect to the source of argon, but most of these can be adequately accounted for. Argon is sensitive to air contamination and volcanic input, and there are indications that its concentration in hydrothermal water of meteoric origin may deviate from that of air saturated ground water.

While there usually are ambiguities with respect to the application any gas geothermometer, they can often be addressed satisfactorily by an interpretative approach which looks for consistency among a variety of y–T and gas ratio grids, and integrates information from other sources, such as stable isotope and noble gas chemistry.

INTRODUCTION

This paper is an outgrowth of a presentation on exploration gas geochemistry I gave at a pre-meeting geochemistry workshop at the 1999 GRC meeting. It has now been 20 years since the first appearance of gas geothermometry techniques, and the subject is still largely viewed with confusion and suspicion. Much of this is due to the complexity of the subject matter and the diversity of techniques employed by the various contributors. On the other hand, while most geochemists would agree that gas geothermometer methods generally work, and are an important component of the explorationist's toolbox, they would also agree that they are often tricky to use and interpret. This work is an attempt to review the state of the art as it applies to exploration geochemistry, with the purpose of clarifying and evaluating the various methods.

Historically, gas geothermometers have evolved through three basic forms: 1) simple thermodynamic and empirical equations, 2) y–T grids, first proposed by Giggenbach (1980) and later popularized by the work of Alfred Truesdell and the late Franco D'Amore, and 3) gas ratio grids, pioneered by the late Werner Giggenbach. This discussion will begin with the thermodynamic and empirical relations, since these constitute the foundation common to all geothermometer methods, then progress through the y–T grid and gas ratio grid methods.

GAS GEOTHERMOMETER EQUATIONS

Most gas geothermometer equations are based upon the thermodynamics of gas species thought to equilibrate in geothermal reservoirs. These thermodynamics are based upon the free energy change of chemical reactions between these species, which can be written in terms of a temperature-dependent equilibrium constant (K) for the reaction. For reactions involving gases these take the form:

$$Log\ K = \Sigma\ log\ P_{products} - \Sigma\ log\ P_{reactants}$$

Strictly speaking, equilibrium constants for gas reactions are in terms of gas fugacities, but for the low pressures in geothermal systems, most fugacity coefficients are near unity and simple partial pressures (P) for gases can be substituted (Henley, Truesdell & Barton, 1984). By convention, reactions are written such that products are favored at higher temperature. Selected log K's for the principal geothermometer reactions are given in Table 1, below.

Table 1: Gas geothermometer equations

FT[1]:	$\log P_{CO2} + 4\log P_{H2} - \log P_{CH4} - 2\log P_{H2O} = 10.76 - 9323/T$
NAH[1]:	$\log P_{N2} + 3 \log P_{H2} - 2 \log P_{NH3} = 11.80 - 5400/T$
HSH[1]:	$3 \log P_{H2S} - \log P_{H2} = 15.71 - 10141/T$ (py-mag)
	$\log P_{H2S} - \log P_{H2} = 4.94 - 2874/T$ (py-pyh)
DAP[2]:	$T = 24775/(2 \log (CH_4/CO_2) - 6 \log (H_2/CO_2) - 3 \log (H_2S/CO_2) - 7 \log P_{CO2} + 36.05)$
H_2S[3]:	$\text{Log } P_{H2S} = 6.05 - 3990/T$
CO_2[4]:	$\text{Log } P_{CO2} = - 8.366 + 0.0168\ T$
CO_2-H_2[5]:	$\log P_{CO2} + 2\log P_{H2} = 16.298 - 8982/T$
CO[6]:	$\log (P_{CO} / P_{CO2}) - \log (P_{H2} / P_{H2O}) = 2.485 - 2248/T$
H_2O[1]:	$\text{Log } P_{H2O} = 5.51 - 2048/T$
z factor[7]:	$\text{Log } z = \log P_{H2O} - 3.041 + 2118/T - \text{Log } T$

All temperatures in degrees Kelvin

References:
1. Giggenbach (1980)
2. D'Amore & Panichi (1980)
3. Giggenbach (1997)
4. Adapted from Giggenbach & Goguel (1989)
5. Henley, Truesdell & Barton (1984)
6. Giggenbach (1987)
7. This study (150°C - 350°C)

Geothermometer temperatures are calculated by converting the gas/steam ratios in the gas analyses to partial pressures, assuming ideal gas behavior, corrected for steam compressibility. The relation can be written:

$$r_{gas} = (P_{gas} / P_{stm}) \cdot z$$

where r_{gas} is the gas/steam ratio and z is the compressibility factor of steam. Many authors simplify geothermometer formulas by ignoring the compressibility factor, but this can lead to errors, particularly at higher temperatures. Steam compressibility equals 0.91 at 200°C and 0.70 at 300°C. The equations for the gas ratio grids in Table 2 assume ideal gas behavior, for example. (See Chapter 5 of Henley, Truesdell & Barton, 1984 for additional background on geothermometer derivations.)

The thermodynamics of a reaction describe the gas pressures at equilibrium, but give no indication as to the speed of the reaction, or reaction kinetics. In reality, some geothermometer reactions appear to be quite rapid while others are comparatively slow. Since chemical reactions tend to occur faster at higher temperature, gas concentrations for reactions too slow to equilibrate in a geothermal reservoir might reflect either partial equilibration or "frozen in" hotter (and presumably deeper) conditions. In other cases, reactions might occur so quickly that the reaction can re-equilibrate during transit between reservoir and surface, leading to a gas geothermometer result that is cooler than reservoir conditions

Fischer-Tropsch Geothermometer (FT)

$$CH_4 + 2H_2O = CO_2 + 4H_2$$

This is perhaps the most popular and heavily used reaction, and it has derivations by numerous authors. The geothermometer has the advantage of being independent of mineral buffers and redox state. The disproportionate influence of hydrogen in the geothermometer equation (factor of 4), however, suggests that it may act as more of a "hydrogen" geothermometer.

Field studies suggest that the reaction is relatively slow to re-equilibrate. Nehring & D'Amore (1984) show that it predicts reservoir temperatures about 30ºC too high at Cerro Prieto. Arnórsson and Gunnlaugsson (1985) give data from a number of fields showing that the geothermometer yields both under- and overestimates of reservoir temperature. They suggest that temperature underestimates may be due to the addition of unequilibrated biogenic methane. Giggenbach (1987) shows evidence that the reaction did not re-equilibrate below about 300ºC in White Island fumaroles. Although White Island is a volcanic system, the kinetics of the reaction would be expected to be the same as in a geothermal environment.

Nitrogen-Ammonia-Hydrogen (NAH)

$$2NH_3 = 3H_2 + N_2$$

Similar derivations of this geothermometer are given by Giggenbach (1980) and Nehring and D'Amore (1984). Like the Fischer-Tropsch reaction, the NAH reaction is independent of redox state and sensitive to hydrogen concentration. From a practical standpoint, the geothermometer's use in an exploration setting is limited due to problems with near-surface ammonia

loss common in fumaroles. Ammonia is the most soluble of the geothermal gases and it readily ionizes to ammonium (NH_4^+) under low pH aqueous conditions, making it the first gas to be lost when liquid water is present in a fumarole system.

Nehring & D'Amore (1984) show closer agreement between NAH and Na-K-Ca temperatures than with FT, but Giggenbach (1987) shows evidence for only very high temperature (>400ºC) equilibration in White Island fumaroles. Lowenstern and others (1999) show that there is a large excess of ammonia in early data from The Geysers field and NAH equilibrium at reservoir temperatures is not consistent with the redox state suggested by other gases. They hypothesize that the excess un-equilibrated ammonia has been added from sedimentary reservoir rocks. In that the NAH geothermometer generally gives reasonable results at The Geysers, this appears to be a case where the geothermometer formulation can give reasonable results even when the component gases are far from equilibrium.

Hydrogen Sulfide – Hydrogen (HSH)

$$3FeS_2 + 2H_2 + 4H_2O = Fe_3O_4 + 6H_2S$$

and

$$FeS_2 + H_2 = FeS + H_2S$$

There are two derivations for this geothermometer, depending on which iron-bearing minerals participate in the reaction (Giggenbach, 1980). In this case, the pyrite-magnetite and pyrite-pyrrhotite mineral pairs reflect different redox states, so some foreknowledge of the probable mineralogy of the system would be needed to determine which geothermometer to apply. The pyrite-magnetite reflects an oxidation state only slightly more reducing than the Fe^{+2}/Fe^{+3} redox buffer favored for reservoirs in volcanic rocks (Giggenbach, 1987). The pyrite-pyrrhotite mineral pair is rarely seen and this version of the HSH geothermometer is rarely used.

By all reports, the pyrite-magnetite version of the geothermometer re-equilibrates quickly and is relatively accurate. Nehring & D'Amore (1984) show good agreement between HSH and Na-K-Ca temperatures at Cerro Prieto. D'Amore & Truesdell (1985) further show good agreement between measured reservoir temperature and the geothermometer for a number of both vapor-dominated and liquid dominated fields.

D'Amore & Panichi Geothermometer (DAP)

$$2CH_4 + 2H_2O = C + CO_2 + 6H_2$$

and

$$CaSO_4 + FeS_2 + 3H_2O + CO_2 = CaCO_3 + 1/3\ Fe_3O_4 + 3H_2S + 7/3\ O_2$$

D'Amore and Panichi (1980) propose an empirical geothermometer based upon reactions between common carbon and sulfur bearing gases and reservoir minerals, and an empirical relation for oxygen fugacity. In a sense, it is a combination of the FT and CO_2-H_2 geothermometers with sulfur controlled by sulfate – sulfide equilibrium. Since it operates on simple gas ratios and an assumed value for the partial pressure of carbon dioxide (P_{CO2}), it is intended to be applied to fumaroles, gas seeps and hot springs alike.

The problem with this geothermometer is that it seems to work in some fields, but not in others. The inclusion of elemental carbon in the reaction suggests that it might be more appropriate for sedimentary reservoirs, although the oxygen fugacities specified in the geothermometer derivation dictate conditions slightly more oxidizing than the Fe^{+2}/Fe^{+3} buffer favored for volcanic hosted systems. The inclusion of sulfate–sulfide equilibrium controlling hydrogen sulfide is questionable, since it generally has been found to be lacking in geothermal systems (e.g., Arnorsson & Gunnlaugsson, 1985; Giggenbach, 1993; Pang & Reed, 1998).

The most critical problem with the geothermometer appears to come from the method for estimating a value of P_{CO2} for the formula. Approximate values of P_{CO2} are selected depending upon the relative concentration of carbon dioxide in the sample. The rules are as follows: In gas analyses where carbon dioxide represents more than 75% of the total gas, P_{CO2} is assigned a value of 1 bar; where it represents less than 75%, it is assigned a value of 0.1 bar. In gases where P_{CO2} is greater than 75% and both hydrogen sulfide and methane are more than twice hydrogen, P_{CO2} is assigned to a value of 10 bars.

The effects of these rules on geothermometer temperatures can be seen in Figure 1. DAP temperatures have been calculated for a hypothetical geothermal gas equilibrated to the FT, H_2S and CO_2 geothermometers at the redox state of the Fe^{+2}/Fe^{+3} buffer, in both reservoir liquid and vapor phases. The open symbols represent DAP temperatures calculated using the actual P_{CO2} of the gas, and the solid symbols represent temperatures calculated using the P_{CO2} estimation rules stated above. While geothermometer temperatures track equilibration temperatures fairly well in both liquid and vapor when actual P_{CO2} is used, the comparison is poor when P_{CO2} is estimated.

Hydrogen Sulfide

$$FeS_2 + FeO + 2H_2O = Fe_2O_3 + 2H_2S$$

Arnorsson and Gunnlaugsson (1985) propose an empirical hydrogen sulfide geothermometer, based upon a correlation with temperature observed in reservoir liquid samples from a number of liquid dominated fields. More recently, Giggenbach (1997) presents a hydrogen sulfide geothermometer based upon pyrite breakdown and a hypothetical fayalite-hematite mineral pair, used as a proxy for the Fe^{+2}/Fe^{+3} redox buffer. Figure 2 shows that the empirical geothermometer compares reasonably well with the thermodynamic geothermometer. This being the case, the empirical geothermometer offers no advantage over the more rigorously constrained thermodynamic one. The correlation does, however, suggest that the geothermometer re-equilibrates at reservoir conditions down to at least 250°C.

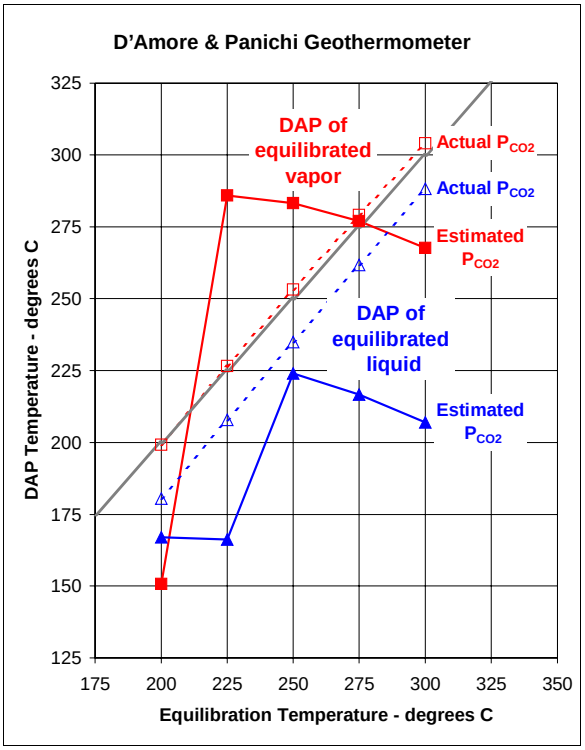

Figure 1: Comparison of the DAP geothermometer (D'Amore & Panichi, 1980) to equilibrated reservoir liquid at –2.8 R_H .

Carbon Dioxide

$$CaCO_3 + K\text{-}mica = CaAl_2\text{-}silicate + K\text{-}feldspar + CO_2$$

Arnorsson and Gunnlaugsson (1985) also propose an empirical carbon dioxide geothermometer, and show that carbon dioxide concentrations in field data are consistent with calcite saturation. Later, Giggenbach (1989) proposed a carbon dioxide geothermometer based upon the thermodynamics of the above reaction. The geothermometer assumes that the reservoir is saturated with respect to calcite and that a neutral-pH mineral assemblage is present. Figure 2 shows that the empirical geothermometer correlates reasonably well with this formulation, again allowing the thermodynamic geothermometer to supersede the empirical one, and suggesting equilibration at reservoir conditions down to 200°C.

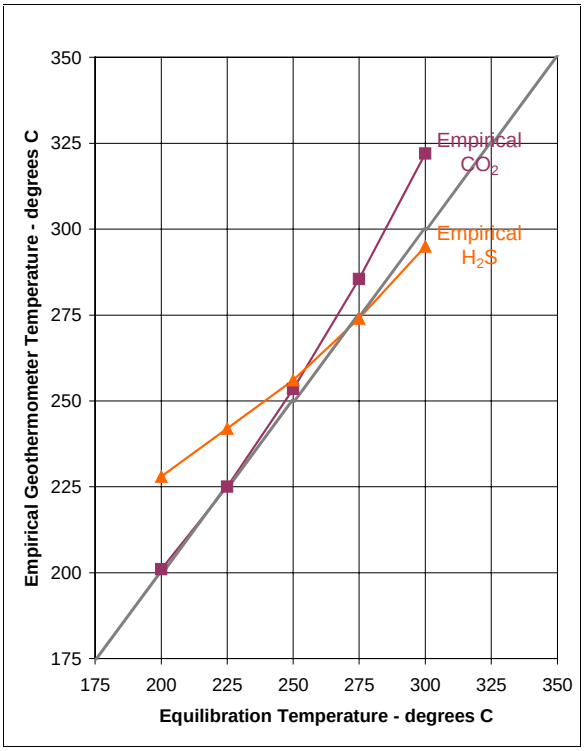

Figure 2: Comparison of CO_2 and H_2S empirical geothermometers (Arnorsson & Gunnlaugsson, 1985) to equilibrated reservoir liquid at -2.8 R_H .

Carbon Dioxide – Hydrogen

$$2H_2O + C = 2H_2 + CO_2$$

Nehring and D'Amore (1984) propose this geothermometer reaction for Cerro Prieto based upon the oxidation of elemental carbon, present in the reservoir as coal. The graphite-carbon dioxide pair represents a redox buffer slightly more reducing than Fe^{+2}/Fe^{+3}, and causes the geothermometer to yield results approximately 25ºC cooler than predicted by the carbon dioxide geothermometer and the Fe^{+2}/Fe^{+3} buffer. However, temperatures indicated by the geothermometer conform reasonably well with the Na-K-Ca temperatures at Cerro Prieto. The geothermometer has not been widely used, however, probably because of the requirement for the presence of graphite (coal) in the reservoir.

Carbon Monoxide

$$CO_2 + H_2 = CO + H_2O$$

Different geothermometers based upon this reaction have been proposed by D'Amore and others (1987) and Giggenbach (1987). Giggenbach (1987) suggests that carbon monoxide in White Island fumaroles re-equilibrates relatively quickly, and D'Amore and others (1987) show good agreement for Larderello steam samples over a 200º to 270ºC temperature range. A complication with using this geothermometer is that a separate (NaOH free) sample is needed for the carbon monoxide analysis.

Y–T Grid Geothermometers

These are so named because data are plotted on a grid of temperature (T) versus "y" value generated by a cross plot of two suitable geothermometer equations. It was recognized early on that many samples of geothermal steam from liquid dominated reservoirs contained more gas than could be generated by equilibrium chemical reactions in the liquid phase. This creates a considerable problem for geothermometers based upon simple equations. In order to address this, Giggenbach (1980) proposed that steam samples contained a mixture of vaporized reservoir liquid and a reservoir vapor in equilibrium with that liquid. The "y" value is defined as the fraction of equilibrium vapor in this mixture. Now, for the geothermometry of any given steam sample, there are two unknowns; temperature and y value. The grid geothermometers provide a graphical solution by plotting two geothermometers on opposing axes and graphically resolving temperature and y on a y–T grid. Figure 3 shows an example of a FT-HSH geothermometer grid.

One serious limitation to the use of gas grids in exploration comes from potential modifications to gas/steam ratio as fumarole steam travels from the reservoir to the surface. Giggenbach (1987) points out that isoenthalpic transport of steam formed over a wide range of reservoir temperatures should exit the surface at about 150ºC. Lower fumarole temperatures suggest cooling (and possible condensation) either by heat conduction or interaction with groundwater. Both of these processes will increase the gas/steam ratio and alter the geothermometer temperature. The gas grid in Figure 3 shows hypothetical examples of this. Besides condensing steam, groundwater addition can remove ammonia due to its relatively high solubility, oxidize hydrogen sulfide, and add atmospheric nitrogen and argon. As demonstrated in Figure 3, fumarole steam affected by these processes can be expected to give anomalous results.

Another limitation is inherent in the y model itself. It is difficult to envision a mechanism by which fumarole steam could be formed by a mixture of completely vaporized reservoir liquid and an equilibrium vapor. At the very least, the model would not be appropriate to steam formed by partial

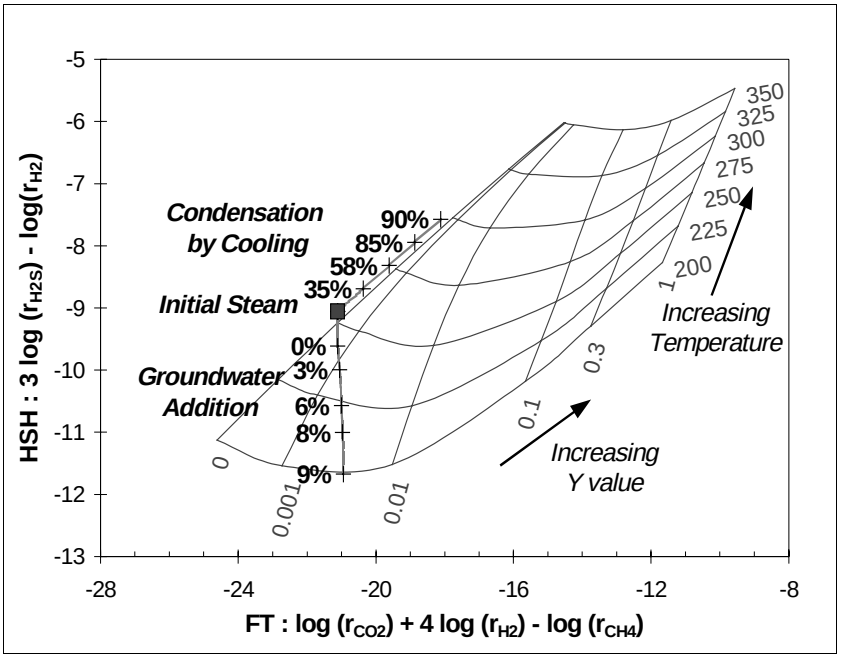

Figure 3: FT-HSH geothermometer grid showing the effect of steam condensation by cooling and by groundwater addition. Percentages show relative mass of steam condensed. The increase in apparent temperature and y value with cooling is due to increased gas/steam ratios. The temperature drop with groundwater addition is due to hydrogen sulfide oxidation.

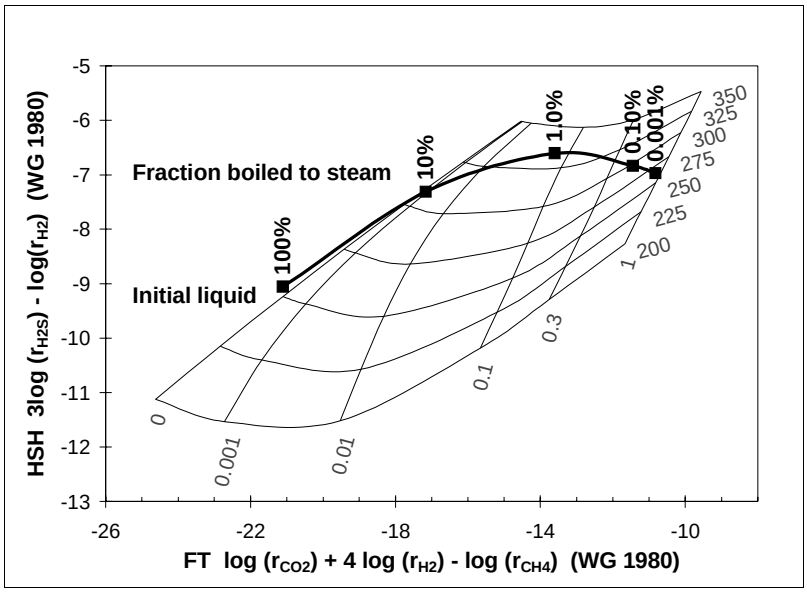

Figure 4: FT-HSH geothermometer grid showing the plot location of steam generated by partial boiling. The y–T model results in a significant temperature overestimate for these samples.

boiling of a reservoir brine, for example. Figure 4 shows where steam generated by partial boiling would plot on an FT-HSH grid; demonstrating that the y model would result in a significant temperature overestimate. The y model is perhaps best suited to well samples in vapor dominated fields, where there is some expectation that the reservoir processes might match the model.

GAS RATIO GRIDS

The gas ratio grids employ a number of strategies to overcome the ambiguities with respect to gas/steam ratio of surface samples and the applicability of the y model. First, the ratio grids are restricted to the gases least soluble in liquid water, so the effects of partial boiling, two-phase reservoir conditions and near surface condensation are minimized. Gases which would be heavily affected by these processes such as hydrogen sulfide and ammonia are not used. Second, argon is used as a proxy for the partial pressure of water vapor (P_{H2O}) under the assumption that the argon concentration in reservoir waters is the same as that in air-saturated groundwater, which isotopes show to be the largest component of hydrothermal waters (Giggenbach & Goguel, 1989). This removes the need for gas/steam ratios, making the grids appropriate for gas seep and hot spring gas samples, as well as steam from fumaroles. Third, a single redox state is assumed, based upon the Fe^{+2}/Fe^{+3} buffer, in order to fix hydrogen fugacities and reduce the Fischer-Tropsch and carbon monoxide geothermometers to simple gas ratios. The buffer appears to control fluid-rock reactions in the volcanic system at White Island (Giggenbach, 1987) and is consistent with the redox state of a number of volcanic hosted hydrothermal systems in New Zealand (Giggenbach & Goguel, 1989) and the Philippines (Giggenbach, 1993). In proposing this buffer a new fluid redox measure based upon the log ratio of hydrogen to steam fugacities, termed R_H is introduced. Fortuitously, the divalent-trivalent iron buffer corresponds to a temperature independent R_H of -2.8 (Giggenbach, 1987), allowing hydrogen fugacities to be fixed at all temperatures. These assumptions reduce the number of expressions used in the gas ratio grids to four; listed for vapor and liquid equilibration conditions in Table 2 below.

Table 2: Gas ratio grid equations

	Sources
$\text{Log } (H_2/Ar)_{vap} = R_H + 6.52$	(1)
$\text{Log } (H_2/Ar)_{liq} = R_H - 3.53 + 0.014\ T$	(1)
$\text{Log } (CO_2/Ar)_{vap} = -7.36 + 0.0168\ T + 2048/T$	(1)
$\text{Log } (CO_2/Ar)_{liq} = -15.10 + 0.0277\ T + 2048/T$	(1)
$\text{Log } (CO/CO_2)_{vap} = R_H + 2.485 - 2248/T$	(2)
$\text{Log } (CO/CO_2)_{liq} = R_H + 0.119 + 0.00296\ T - 2248/T$	(2)
$\text{Log } (CH_4/CO_2)_{vap} = 4\ R_H + 0.135 + 5181/T$	(2)
$\text{Log } (CH_4/CO_2)_{liq} = 4\ R_H - 2.231 + 0.00291\ T + 5181/T$	(2)

All temperatures in degrees Kelvin

(1) adapted from Giggenbach & Goguel (1989)
(2) adapted from Giggenbach (1987)

$CO_2/Ar - H_2/Ar$

The assumption of a single fixed redox state (or R_H) for all hydrothermal systems allows the temperature-dependent water dissociation reaction to be used as a hydrogen geothermometer. Combined with argon as a measure of P_{H2O}, the hydrogen and carbon dioxide geothermometers have been combined to yield the

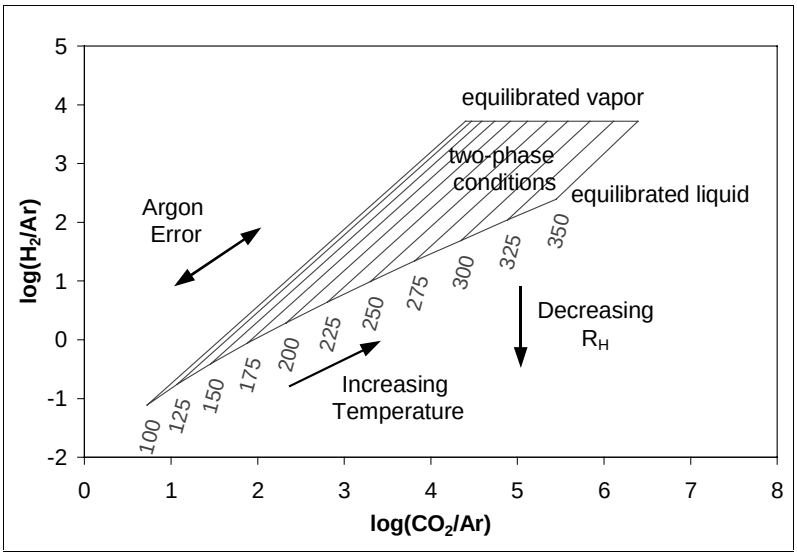

Figure 5: CO_2/Ar – H_2/Ar gas ratio grid. The grid shifts vertically downward at lower R_H conditions

gas ratio grid illustrated in Figure 5, after Giggenbach & Goguel (1989).

The grid assumes the presence of carbonate for the carbon dioxide geothermometer and R_H -2.8 for the hydrogen geothermometer. The liquid equilibration line represents the equilibration for gas in an entirely aqueous environment, whereas the steam equilibration line represents gas equilibration in a vapor phase at the same argon gas concentration. Samples plotting above the liquid equilibration line indicate alternatively equilibration under vapor conditions, such as in a steam cap, or possible argon loss, or an R_H greater than -2.8. Samples plotting below this line indicate alternatively hydrogen re-equilibration at lower temperatures, argon gain or R_H less than -2.8. If desired, the grid can be shifted to reflect equilibration at a different redox state.

The argon ratio grid geothermometers suffer from problems and ambiguities unique to argon. First, argon concentrations are strongly affected by air contamination in gas samples. Even when reagents are used to stabilize contaminant air so that it can be accurately measured and accounted for, argon derived from air often overwhelms the argon from the hydrothermal source and can create significant errors in the corrected argon concentration. Uncertainty in argon can best be reduced by careful sampling techniques and by the collection of more than one sample from any one source. Unfortunately, argon error creates a trend nearly parallel to the liquid equilibration line, adversely affecting the resolution of temperature on the grid.

Second, stable isotopes show that many geothermal systems contain significant primary magmatic water, or "andesitic water" (Giggenbach, 1992), which generally contains much lower argon concentration than groundwater. Giggenbach (1993) proposes a correction factor for magmatic water, based upon the fraction of andesitic water in the sample, as determined by stable isotopes:

$$\boldsymbol{Log\ (H_2/Ar) = Log\ (\ r_{H2} / r_{Ar}\ ) - log\ (\ 1 - x_a\ )}$$

where x_a is the fraction of andesitic water.

There is a final concern with respect to the actual argon concentrations of hydrothermal waters. Norman and Moore (1999) show that although most groundwaters are at saturation with respect to argon at surface conditions, fluid inclusions from many ancient and active hydrothermal systems contain significantly more argon than air-saturated water. Single phase liquid samples from the Tiwi field, Philippines, for example, show about ten times more argon than in air-saturated water, while also showing atmospheric nitrogen-argon ratios. On the other hand, Mazor and Truesdell (1984) show that samples from Cerro Prieto wells contain noble gas ratios consistent with air saturated water, but at concentrations as low as one tenth that predicted for air saturated water. More work is needed to quantify these differences, but it appears that offsets in argon concentration by as much as a log unit from the benchmark air-saturated water value might be expected.

Despite these uncertainties, the CO_2/Ar–H_2/Ar ratio grid has been generally found to give good results, and the ability to apply it a variety of sample sources makes it quite versatile.

CO/CO_2 – CH_4/CO_2

The grid based upon these two geothermometers is

presented in Figure 6, after Giggenbach and Goguel (1989). Typically, few samples plot within the narrow field of equilibration with this combination, probably because the grid pairs the relatively fast acting carbon monoxide geothermometer with the slow FT reaction. The R_H-dependence of both gas ratios can make the grid useful in the determination of R_H, however, which can be helpful in distinguishing surface manifestations of volcanic origin from hydrothermal ones.

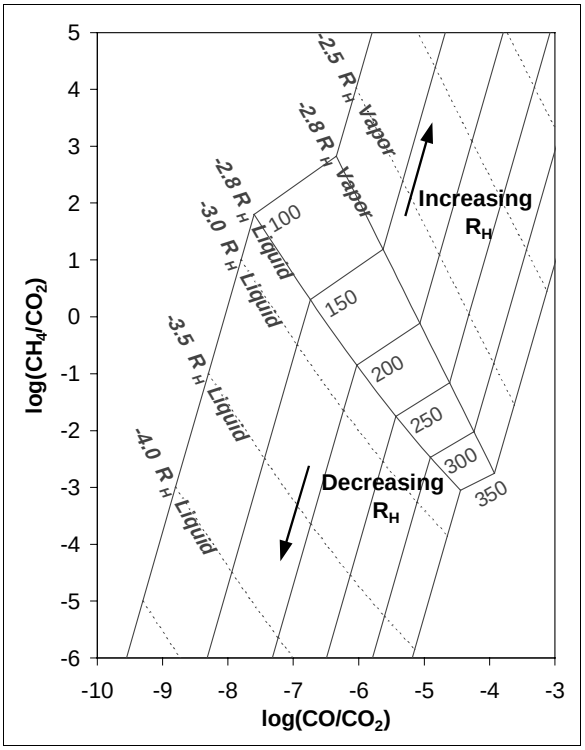

Figure 6: CO/CO_2 – CH_4/CO_2 gas ratio grid. The area between the –2.8 R_H vapor and liquid lines is the field of equilibration for the Fe^{+2}/Fe^{+3} redox buffer.

Other combinations of these ratio geothermometers include CO/CO_2–H_2/Ar (Giggenbach & Glover, 1992) and H_2/Ar–CH_4/CO_2 (Giggenbach, 1993), both of which are similarly R_H dependent. The former pair is perhaps the more useful, since it pairs geothermometers of similarly rapid equilibration. In cases of a lengthy transit time from source to surface, this pair might even be expected to give temperatures that are slightly low. Giggenbach and Glover (1992) show good correspondence between this grid and aqueous geothermometers for moderate source temperature (200ºC) hot springs at Rotorua.

The H_2/Ar – CH_4/CO_2 grid suffers the same problem as the CO/CO_2 – CH_4/CO_2 grid, in that it pairs an even faster geothermometer (H_2/Ar) with the slow CH_4/CO_2 geothermometer (Giggenbach, 1987). Giggenbach (1993) found this grid useful in evaluating the redox state of a set of Philippine hydrothermal and volcanic systems.

CONCLUSIONS

Two factors critical to the success of a geothermometer in a particular setting are the presence of specified mineral reactants and buffers, and the speed of equilibration. Studies suggest that the H_2, CO, HSH, H_2S, CO_2 and CO_2-H_2 geothermometers can be expected to equilibrate in the range of commercial reservoir temperatures (i.e., 200ºC to 300ºC), whereas FT is marginal and NAH is probably too slow. These last two may also be thrown off by generation of biogenic methane and ammonia in sedimentary-hosted reservoirs. Instances of success of the NAH, and DAP geothermometers are likely fortuitous, suggesting that detailed geochemical studies, like that by Lowenstern and others (1999), are needed when comparing geothermometer results with downhole temperature data.

The affects of steam condensation on y–T grid geothermometers essentially limits their use to superheated fumaroles. With the y–T grids, caution is needed when matching geothermometers of differing equilibration rates and redox buffers, and in applying the y model. Nevertheless, conformance in geothermometer temperature and y value among different grids can be taken to indicate likely equilibration at the source. Depending upon how closely the suspected mechanism of steam formation conforms to the y model, these temperatures could, within reason, be extrapolated to reservoir conditions. A lack of conformance, or gas analyses that plot off the grids, suggest alternatively a lack of equilibration, a different steam formation mechanism or different redox conditions.

The gas ratio grids offer practical advantages over y–T grids in that they can be applied to gases from hot springs and gas seeps, as well as fumaroles, and can provide information about the oxidation state of the system. This is not to say that ratio grids should replace y–T grids; they are simply more arrows in the geochemist's quiver. The gas ratio grids also clarify and simplify an interpretation by reducing the considerations of y to simply whether or not there is evidence of a reservoir steam phase, and by helping to identify an unusual redox state. The central role of argon and the pairing of fast and slow geothermometers appear to be the most serious drawbacks of the ratio grids. Most problems associated with argon can be dealt with, and the argon ratio grids appear to give good results. In order to minimize ambiguities as to the source of argon, sampling strategies are needed to avoid air

contamination, and make available additional analyses, such as water and noble gas isotopes.

ACKNOWLEDGEMENTS

The author would like to thank Mitchel Stark, Richard Gunderson and Pat Dobson for helpful reviews of this paper.

REFERENCES

Arnorsson, S., 1985, Gas pressures in geothermal systems; Chemical Geology, Vol. 49, pp. 319-328.

Arnorsson, S. & Gunnlaugsson, E., 1985, New gas geothermometers for geothermal exploration – calibration and application; Geochim. Cosmochim. Acta., Vol. 49, pp 1307-1325.

D'Amore, F. & Panichi, C., 1980, Evaluation of deep temperatures of hydrothermal systems by a new gas geothermometer; Geochim. Cosmochim. Acta, Vol. 44, pp. 549-556.

D'Amore, F. & Truesdell, A.H., 1985, Calculation of geothermal reservoir temperatures and steam fractions from gas compositions; Trans. Geothermal Res. Council, Vol. 9, Part 1, August 1985, pp 305-310.

D'Amore, F., Fancelli, R., Saracco, L. & Truesdell, A.H., 1987, Gas geothermometry based on CO content – application in Italian geothermal fields; Proc. 12th Workshop Geothermal Reservoir Eng., Jan. 1987, Sanford Univ., Stanford, Calif.

Giggenbach, W. F., 1980, Geothermal gas equilibria; Geochem Cosmochem Acta, V. 44, pp 2021-2032.

Giggenbach, W.F., 1987, Redox processes governing the chemistry of fumarolic gas discharges from White Island, New Zealand; Applied Geochemistry, Vol. 2, pp. 143-161.

Giggenbach, W.F. & Goguel, R.L., 1989, Collection and analysis of geothermal and volcanic water and gas discharges; DSIR report CD 2401, 4th ed., Pentone, NZ, dated Oct. 1989

Giggenbach, W.F., 1992, Magma degassing and mineral deposition in hydrothermal systems along convergent plate boundaries, SEG distinguished lecture; Economic Geology, Vol. 87, pp. 1927-1944.

Giggenbach, W.F. & Glover, R.B., 1992, Tectonic regime and major processes governing the chemistry of water and gas discharges from the Rotorua geothermal field, New Zealand; Geothermics, Vol. 21, No. 1/2, pp. 121-140.

Giggenbach, W.F., 1993, Redox control of gas compositions in Philippine volcanic-hydrothermal systems; Geothermics, Vol. 22, No. 5/6, pp 575-587.

Giggenbach, W.F. , 1997, The origin and evolution of fluids in magmatic-hydrothermal systems, in Geochemistry of Hydrothermal Ore Deposits, 3rd edition, H.L. Barnes ed., John Wiley & Sons, NY, June 1997.

Henley, R.W., Truesdell, A.H. & Barton, P.B., 1984, Fluid-Mineral Equilibria in Hydrothermal Systems; Reviews in Economic Geology, Vol. 1, Society of Economic Geologists, El Paso, TX.

Lowenstern, J.B., Janik, C.J., Fahlquist, L.S. & Johnson, L.S., 1999, Gas and isotope geochemistry of 81 steam samples from wells in The Geysers Geothermal Field, Sonoma and Lake Counties, California, U.S.A.; USGS Open-File Report 99-304.

Mazor, E. & Truesdell, A.H., 1984, Dynamics of a geothermal field traced by noble gases: Cerro Prieto, Mexico; Geothermics, Vol. 13. pp. 91-102.

Nehring, N.L. & D'Amore, F., 1984, Gas chemistry and thermometry of the Cerro Prieto, Mexico, geothermal field: Geothermics, Vol. 13, pp. 75-89.

Norman, D.I. & Moore, J.N., 1999, Methane and excess N_2 and Ar in geothermal fluid inclusions; Proc. 24th Workshop Geothermal Reservoir Eng., Jan. 1999, Sanford Univ., Stanford, Calif., pp. 196-202.